We are IntechOpen,
the world's leading publisher of
Open Access books
Built by scientists, for scientists

6,900
Open access books available

185,000
International authors and editors

200M
Downloads

154
Countries delivered to

Our authors are among the

TOP 1%
most cited scientists

12.2%
Contributors from top 500 universities

BOOK CITATION INDEX
CLARIVATE ANALYTICS
INDEXED

WEB OF SCIENCE™

Selection of our books indexed in the Book Citation Index
in Web of Science™ Core Collection (BKCI)

Interested in publishing with us?
Contact book.department@intechopen.com

Proof of the Energetic Efficiency of Fresh Air, Solar Draught Power Plants

Radu D. Rugescu

Additional information is available at the end of the chapter

1. Introduction

The thermal draft principle is currently used in exhaust chimneys to enhance combustion in domestic or industrial heating installations. An introductory level theory of gravity draught in stacks was issued by the old German research institute for heating and ventilation (Hermann-Rietschel-Institut) in Charlottenburg, in a widely translated reference book (Raiss 1970). Technological and practical aspects of air draught management are clearly exposed in this works, but a wide-predicting theory still lacks. As early as in 1931 a surprisingly advanced proposal to use thermal draught as a propelling system to generate electricity from solar energy was forwarded by another German researcher (Günter 1931). Major advancements in convective flows prediction during the last decades of the 20th century were accompanied by a series of publications and we cite first the basic book due to a work from Darmstadt (Unger 1988). The related topic of convective *heat transfer*, often involved in thermal draught, was also intensively studied and the advanced results published (Jaluria 1980; Bejan 1984). With these records the slippery analytical theory of natural gravity draught was set well under control. Thermal energy from direct solar heating is regularly transformed into electricity by means of steam turbines or Stirling closed-loop engines, both with low or limited reliability and efficiency (Schiel et al. 1994, Mancini 1998, Schleich 2005, Gannon & Von Backström 2003, Rugescu 2005). Steam turbines are driven through highly vaporised water into tanks heated on top of supporting towers, where solar light is concentrated trough heliostat mirror arrays. High maintenance costs, the low reliability and large area occupied by the facility had dropped the interest into such renewable energy power plants. The alternative to moderately warm the fresh air into a large green house and draught it into a tower, checked only once, gave also a very low energetic efficiency, due to the modest heating along the green house. This existing experience has fed up a visible reluctance towards the solar tower power plants (Haaf 1984).

However, a simple and efficient solution exists which is here demonstrated by means of energy conservation. This method provides a superior energetic efficiency with moderate costs and a high reliability through simplicity. It consists of optimally heating the fresh-air by means of a mirror array concentrator and an efficient solar receiver, and accelerating it further in the tall towers through gravity draught (Fig. 1, Rugescu 2005).
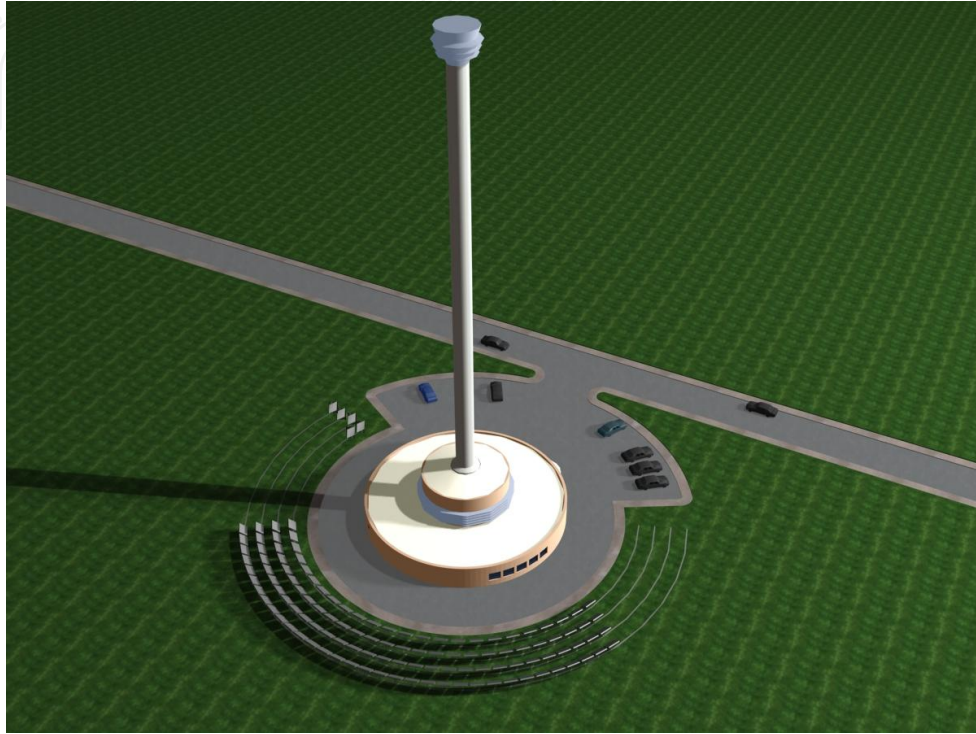

Figure 1. Project of the ADDA solar array gravity draught accelerator.

This genuine combination has already a history of theoretical study (Rugescu 2005) and an incipient experimental history too (Rugescu et al. 2005). First designed for air acceleration without any moving parts or drivers with application to infra-turbulence aerodynamics and aeroacoustics, the project was further extended for green energy applications along a series of published studies (Rugescu et al. 2006, Rugescu 2008, Rugescu et al. 2008, Rugescu et al. 2009, Rugescu et al. 2010, Cirligeanu et al. 2010, Rugescu et al. 2011a, Rugescu et al. 2011b, Rugescu 2012, Rugescu et al. 2012a, Rugescu et al. 2012b). The demonstration of the high draught tower energetic efficiency provided below is expected to convince the skeptics and to bolster again the direct solar energy exploitation in tall tower power plants (Rugescu et al. 2012 b).

2. Gravity-draught accelerator modeling

A schematic diagram of a generic draught tower is drawn in Fig. 2. The fresh air in its ascending motion up the tower, due to the gravity draught, is first absorbed, from the immobile atmosphere (w_0=0), through the symmetrically positioned air intakes at the level designated as

station "0", close to the ground (Fig. 2). It turns upright along the curved intake and accelerates afterwards to the velocity w_1 through the laminator. It then enters the solar heater, or solar receiver, at station "1" into the stack. Due to warming and dilatation into that receiver by absorption of the thermal flux $\dot{q}$ it accelerates further to velocity w_2 at receiver exit "2", from where after the heat transfer to the walls is small and is supposedly neglected and the light air is draught upwards with almost constant velocity up to the upper exit of the tower "3", under the influence of the differential gravity effect of almost constant intensity g between the inner and outer zone of the atmosphere. The tower secures an almost one-directional flow and consequently the problem will be treated here as one-dimensional.

The ideal gas behavior under the influence of a gravity field of intensity g, flowing upward with the local velocity w into a vertical duct of cross area A and subjected to a side wall heating by a thermal flux $\dot{q}$ is fully described by the 3-D conservation laws of mass, impulse, energy, by the equation of state and by the physical properties of the gas, the air in particular.

The air flow of the material, infinitesimal control volume $dV \equiv A(x)\,dx$ into the vertical pipe of variable cross area A and subjected to side heating by a thermal flux $\dot{q}(t, x)$ is described by the conservation laws of mass, impulse and energy successively:

$$\frac{dM_V}{dt} \equiv \frac{d}{dt}\int_{dV}\rho dV = \frac{\partial}{\partial t}\int_{dV}\rho dV - \oint_{\partial dV} \boldsymbol{w}\cdot\boldsymbol{n}\,\rho dS = 0 \tag{1}$$

$$\frac{d\boldsymbol{H}_V}{dt} \equiv \frac{d}{dt}\int_{dV}\rho \boldsymbol{w}dV = \frac{\partial}{\partial t}\int_{dV}\rho \boldsymbol{w}dV - \oint_{\partial dV} \boldsymbol{w}\,\boldsymbol{w}\cdot\boldsymbol{n}\,\rho dS = \oint_{\partial dV} \boldsymbol{\tau}\cdot\boldsymbol{n}\,dS + \int_{dV}\rho \boldsymbol{g}\,dV \tag{2}$$

$$\frac{dE_V}{dt} \equiv = \frac{\partial}{\partial t}\int_{dV}\left(e + \frac{w^2}{2}\right)\rho dV - \oint_{\partial dV}\left(e + \frac{w^2}{2}\right)w_n \rho dS = \oint_{\partial dV}\boldsymbol{\tau}\cdot\boldsymbol{n}\cdot\boldsymbol{w}\,dS + \oint_{\partial dV}\dot{q}\,dS + \int_{dV}\boldsymbol{g}\cdot\boldsymbol{w}\,\rho\,dV \tag{3}$$

where e and k are the intensive inner energy and kinetic energy of the gas, respectively. The stress tensor τ acts on the walls only, meaning the boundary of the control volume.

The computational solution of the stack flow further depends on the initial and limit conditions that must fit the physical process of thermal draught (Bejan 1984) and may be managed in simple thermodynamic terms. In its general form, the dynamic equilibrium of the stack flow was first debated in a dedicated book (Unger 1988), with emphasize on the static pressure equilibrium within and outside the stack at the openings, the key of the entire stack problem. The one-dimensional steady flow assumption with negligible friction was accounted and we add the proofs that this approach is consistent with the problem. In that regard we analyze in a new way the flow with friction losses, estimate their magnitude and add a different accounting for compressibility at entrance. Our point of view faintly modifies the foregoing results regarding the compressibility of the air during inlet and exit acceleration, still consists of a necessary improvement.
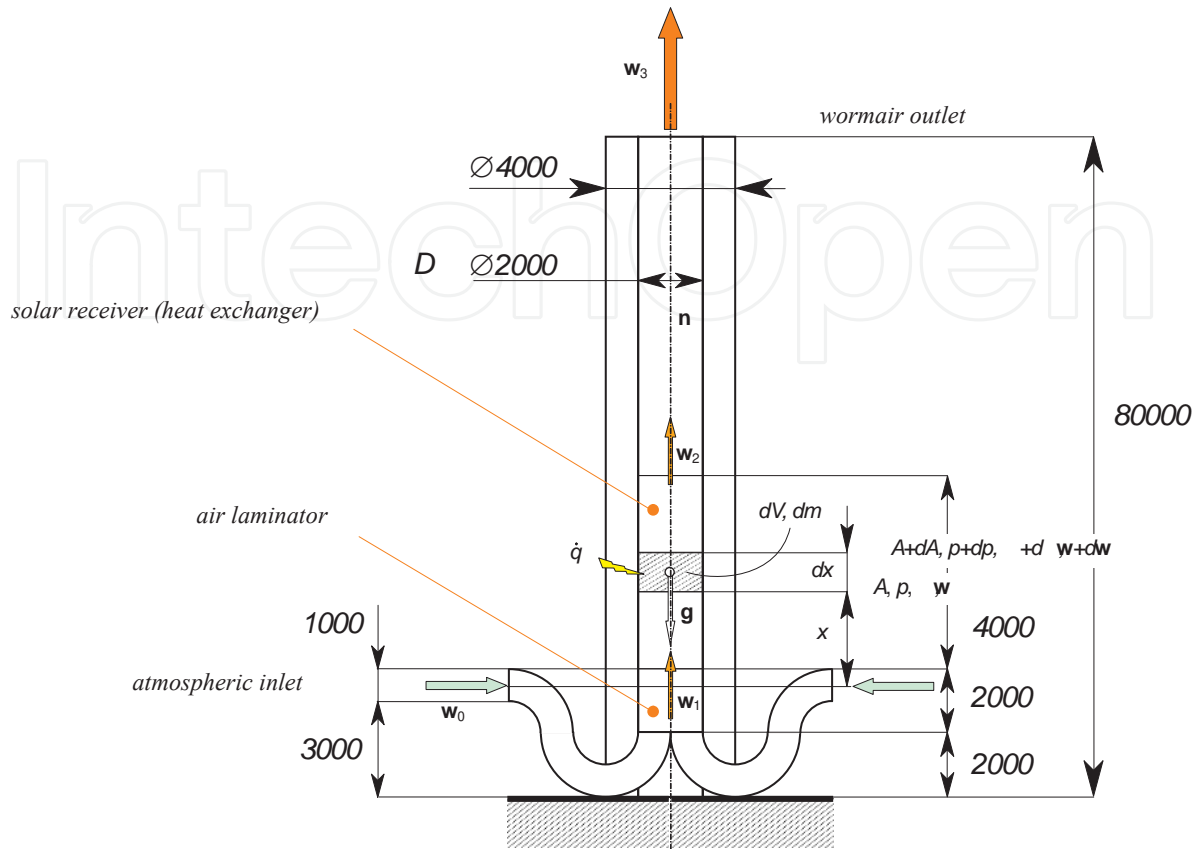
Figure 2. Control volume into a generic stack.

The aerostatic influence of the gravitation is then given by the pressure gradient equation inside (density ϱ) and outside (density ϱ_0) the tower,

$$\frac{\mathrm{d}\,p}{\mathrm{d}\,z}=-g\,\rho,\quad \frac{\mathrm{d}\,p}{\mathrm{d}\,z}=-g\,\rho_0 \tag{4}$$

The right hand term in these equations is nothing but the slope to the left of the vertical in each pressure diagram from Fig. 3.

This means that the inner pressure in the stack (left, doted line) is decreasing less steeply and remains closer to the vertical than the outer pressure of the atmosphere. The dynamic equilibrium is established when, following a series of transforms, the stagnation pressures inside and outside become equal (Fig. 3). While the air outside the stack preserves immobile and due to the effect of gravitation its pressure decreases with altitude from $p_{\mathrm{ou}}(0){\equiv}p_0$ at the stack's pad to $p_{\mathrm{ou}}(\ell)$- at the tip of the stack "4", the inner air is flowing and consequently its pressure p_{in} varies not only by gravitation but also due to acceleration and braking along the 0-1-2-3-4 cycle.

Figure 3. Dynamics of the gravitation draught.
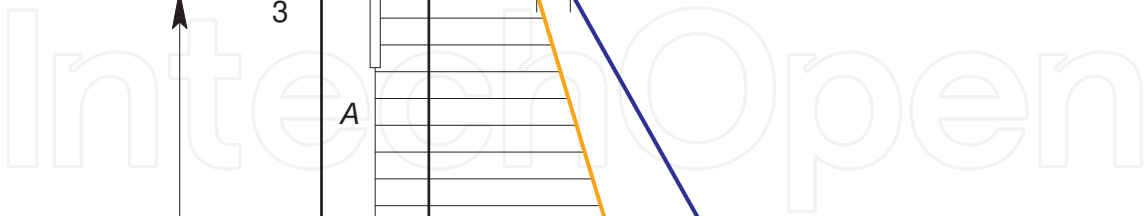
Under the assumption of a slender tower with constant cross area A, meaning a unidirectional flow under an established, steady-state condition with friction under laminar behavior or developed turbulence, the conservation laws for a finite control volume from stage "1" to station "z" are further developing into the conservation of mass,

$$\rho w = const. \tag{5}$$

and energy for the compressible flow, with the assumption $\rho_1 \approx \rho_0$,

$$\frac{p_0}{\rho_0} = \frac{p_1}{\rho_1} + \frac{\kappa - 1}{2\kappa} w_1^2 \leftrightarrow p_0 = p_1 + \frac{k}{2} \frac{\dot{m}^2}{\rho_0 A^2} \tag{6}$$

for the entrance into the stack. In other words the air acceleration takes place at tower inlet between 0-1 as governed by the energy compressible equation with constant density ρ_0 along,

$$p_1 = p_0 - \frac{\Gamma}{2} \cdot \frac{\dot{m}^2}{\rho_0 A^2} \tag{7}$$

where A is the cross area of the inner channel, $\dot{m}$ the mass flow rate, constant through the entire stack (steady-state assumption) and the thermal constant Γ with the value for the cold air

$$\Gamma \equiv \frac{\kappa - 1}{\kappa} = 0.28826 \tag{8}$$

The air is warmed in the heat exchanger/solar receiver between the sections 1-2 with the heat q per kg with dilatation and acceleration of the airflow, accompanied by the "*dilatation drag*" pressure loss. Considering again $A=const$ for the cross-area of the heating zone too, the continuity condition shows that the variation of the speed is simply given by

$$w_2 = w_1 / \beta \tag{9}$$

The impulse equation gives now the value of the pressure loss due to air dilatation,

$$p_2 + \frac{\dot{m}^2}{\rho_2 A^2} = p_1 + \frac{\dot{m}^2}{\rho_0 A^2} - \Delta p_R \tag{10}$$

where a possible pressure loss into the heat exchanger Δp_f due to friction is considered. Once the dilatation drag is thus perfectly identified, the total pressure loss Δp_Σ from pad's outside up to the exit from the heat exchanger results as the sum of the inlet acceleration loss (7) and the dilatation loss (10),

$$p_2 = p_0 - \frac{\dot{m}^2}{2\rho_0 A^2} + \frac{\dot{m}^2}{\rho_0 A^2} - \frac{\dot{m}^2}{\rho_2 A^2} - \Delta p_R \equiv p_0 - \Delta p_\Sigma, \tag{11}$$

equivalent to

$$p_2 = p_0 - \frac{\dot{m}^2}{\rho_0 A^2} \cdot \frac{r(2-\Gamma) + \Gamma}{2(1-r)} - \Delta p_R \tag{12}$$

The gravitational effect (4) continues to decrease the value of the inner pressure up to the exit rim of the stack, where the inner pressure becomes

$$p_3 \equiv p_2 - g\rho_2 \ell = p_0 - \frac{\dot{m}^2}{\rho_0 A^2} \cdot \frac{r(2-\Gamma) + \Gamma}{2(1-r)} - \Delta p_R - g\rho_2 \ell \tag{13}$$

Either the impulse equation in the form

$$\frac{\dot{m}}{A}(w_2 - w_1) = p_1 - p_{in}(z) - \Delta p_f - g\rho_2 z, \tag{14}$$

or the energy equation in the form

$$\frac{\kappa}{\kappa-1}\left(\frac{p_{in}}{\rho}-\frac{p_1}{\rho_1}\right)+\frac{w^2-w_1^2}{2}=\left(\frac{\dot{q}}{\dot{m}}P_{in}-g\right)(z-z_1) \tag{15}$$

appears for the receiver, heated zone, and

$$p_2-p_{in}(z)=\frac{\kappa-1}{\kappa}g\rho_2(z-z_2),\ \ p_2-p_3=\frac{\kappa-1}{\kappa}g\rho_2(z_3-z_2) \tag{16}$$

for the free ascending flow above the receiver, with P_{in} for the perimeter length of the inner channel walls.

At the upper exit from the stack the gas is diluting and braking into the still atmosphere, thus the compressible Bernoulli equation applies,

$$p_3+\frac{\kappa-1}{\kappa}\frac{\rho_2}{2}w_3^2=p_{4'},\ \ \ \ p_3+\frac{\kappa-1}{\kappa}\frac{\rho_2^2w_3^2A^2}{2\rho_2A^2}=p_{4'} \tag{17}$$

when constant density during this process is assumed again. The pressure variation at stack's exit is very small and this ends in the fact that other simplifying hypotheses do not give results consistent with the physical phenomena.

Modifying eq. (14) the inner static pressure at stage z with friction is immediately delivered into the following expression

$$p_{in}(z)=p_{ou}(z)-\frac{1+r}{2(1-r)}\cdot\frac{\dot{m}}{\rho_0A^2}-\Delta\,p_f(z)+g\,\Delta\rho\,z \tag{18}$$

where the relative heating of the air is expressed in terms of densities,

$$r\equiv\frac{\rho_0-\rho_2}{\rho_0}=1-\frac{\rho_2}{\rho_0}\equiv1-\beta \tag{19}$$

with a given control value for

$$\beta = \frac{\rho_2}{\rho_0} < 1 \tag{20}$$

Using eq. (17) the static pressure of the exhausted air becomes

$$p_4(\ell) = p_{ou}(\ell) - \left[\frac{1+r-\Gamma}{1-r} \cdot \frac{\dot{m}^2}{2\rho_0 A^2} + \Delta p_f(\ell) - g \Delta \varrho \ell \right] \tag{21}$$

which is used in the equilibrium condition as follows.

The values of the pressures and velocities into the main sections result from the equilibrium condition of the pressures above the upper exit, where the inner $p_4(\ell)$ and the outer $p_4^* \equiv p_{ou}(\ell)$ values should be equal. That means the square bracket in (21) is set to zero.

In this way (Unger 1988, Rugescu 2005, Rugescu et al. 2005), the mass flow rate through the stack mainly depends on the relative heating of the air, expressed in terms of densities, and results when the pressure difference between the interior and the exterior of the tower exit recovers by dynamic braking of the air (Fig. 3).

$$\frac{\Delta p(\ell)}{g \varrho_0 \ell} \equiv \frac{1+r-\Gamma}{1-r} \cdot \frac{\dot{m}^2}{2g \ell \varrho_0^2 A^2} + \frac{\Delta p_f(\ell)}{g \varrho_0 \ell} - r = 0 \tag{22}$$

For negligible friction losses ($\Delta p_f(\ell) = 0$) the equilibrium mass flow rate becomes

$$R^2 \equiv \frac{\dot{m}^2}{2g \ell \rho_0^2 A^2} = \frac{r(1-r)}{1+r-\Gamma} \tag{23}$$

slightly higher than the predicted value of the previous models (Unger, 1988).

When the friction losses are considered, the actual value for the quadratic mass flow rate results from the second degree equation (22-12) which gets the form,

$$a \left(\frac{\dot{m}}{\dot{m}_\ell} \right)^2 + b \frac{\dot{m}}{\dot{m}_\ell} - r = 0 \tag{24}$$

where at the nominator a reference free-fall mass flow rate appears,
$\dot{m}_\ell = w_\ell \rho_0 A$,

based on the Torricelli free-fall velocity

$$w_\ell^2 = 2g \ell, \tag{25}$$

with the constants

$$a = \frac{r/R}{w_\ell^2 \rho_0^2 A^2}, \quad b = \frac{32\,v_0}{AD^2 g \rho_0}\left(\frac{T_w}{T_c}\right)^{1.7} \tag{26}$$

For an example slender, tall stack with the inner channel of elongation $\ell/D = 70/2$ the resulting contribution of friction is really small,

$b/a = 2\%$,

meaning that the difference from the frictionless flow is actually smaller than 0.5 ‰. Consequently the non-friction result in (23-13) should be considered as accurate. Its quadratic form shows the known fact that the heating of the inner air presents an optimal value and there exist an upper limit of the heating where the flow in the stack ceases.

Formula (23-13) shows that the non-dimensional quadratic mass flow rate R^2 is in fact simply the squared ratio of the exhibited stack entrance speed w_1 over the free-fall speed w_ℓ, due to the constant cross area of the stack,

$$R^2(r) \equiv \left(\frac{w_1}{w_\ell}\right)^2 = \frac{r(1-r)}{1+r-\Gamma}, \tag{27}$$

and is given by

$$R^2(r) \equiv \frac{\dot{m}^2}{w_\ell^2 \rho_0^2 A^2} = \frac{r(1-r)}{1+r-\Gamma} \tag{28}$$

The entrance speed exhibits a maximum at the theoretically optimal heating r_{opt},

$$dR^2/dr = 0, \quad r_{opt}^2 + 2(1-\Gamma)r_{opt} - (1-\Gamma) = 0, \tag{29}$$

namely

$$r_{opt} = -(1-\Gamma) + \sqrt{(1-\Gamma)(2-\Gamma)} \tag{30}$$

The optimal heating for the standard air appears at a relative density reduction

$$r_{opt} \equiv (\rho_0 - \rho)/\rho_0 = 0.392033 \rightarrow R^2(r_{opt}) = R_{max}^2, \tag{31}$$

meaning an equal increase of the absolute temperature of $(1+r)$ times, when the normal air temperature should be raised with around 120ºC above 27ºC to achieve a maximal dis-

charge. Due to Archimedes' effect (Unger, 1988), these values are an optimal response to the craft balance between the drag of the inflated hot air and its buoyant force.

A slightly improved model is delivered when the following conditions at the upper exit are introduced, starting from equation (19). The constant density assumption along the upper stack $\rho_2 = \rho_3 = \rho_4$ was used. Recovery of the static air pressure, previously considered through a compressible process governed by the Bernoulli equation (Rugescu 2005)

$$p_4{}^* = p_3 + \Gamma \frac{\dot{m}^2}{2\rho_2 A^2} \tag{32}$$

is here replaced with the condition (Unger 1988) of an isobaric exit $p_4{}^* = p_3$ which, considered into (19) for replacing p_3, ends in the equilibrium equation

$$p_4{}^* = p_0 - \frac{\dot{m}^2}{\rho_0 A^2} \cdot \frac{r(2-\Gamma) + \Gamma}{2(1-r)} - \Delta p_R - g\rho_2 \ell \tag{33}$$

This means that the dynamic equilibrium is re-established when the stagnation pressure from inside the tower equals the one from outside, at the exit level,

$$p_4{}^* \equiv p_{in}(\ell) = p_{ou}(\ell) \equiv p_0(0) - g\rho_0 \ell \tag{34}$$

This equation is the end element that allows determining the equilibrium value of the air mass flow rate passing through the stack. Equaling (20) and (21),

$$p_0 - g\rho_0 \ell \equiv p_0 - \frac{\dot{m}^2}{\rho_0 A^2} \cdot \frac{r(2-\Gamma) + \Gamma}{2(1-r)} - \Delta p_R - g\rho_2 \ell \tag{35}$$

Reducing by the quotient $g\varrho_0 \ell$ the equilibrium equation appears in the form

$$\frac{\Delta p(\ell)}{g\,\varrho_0\,\ell} \equiv \frac{1+r-\Gamma}{1-r} \cdot \frac{\dot{m}^2}{2g\,\ell\,\varrho_0{}^2 A^2} + \frac{\Delta p_R(\ell)}{g\,\varrho_0\,\ell} - r = 0 \tag{36}$$

Depending on the construction of the heat exchanger the drag largely varies. For simple, tubular channels the pressure loss due to frictions stands negligible (Rugescu et al. 2005a, Rugescu 2005, Rugescu et al 2005b) and the reduced mass flow rate (RMF) results from the simple equation

$$R^2 \equiv \frac{\dot{m}^2}{2g\,\ell\,\rho_0{}^2 A^2} = \frac{r \cdot (1-r)}{r(2-\Gamma) + \Gamma} \tag{37}$$

It gives an alternative to the previous solution of Unger (Unger 1988)

$$R^2 = \frac{r(1-r)}{1+r}, \tag{38}$$

or to the one from above (Rugescu et al. 2005a)

$$R^2 = \frac{r(1-r)}{1+r-\Gamma}, \tag{39}$$

and gives optimistic values in the region of smaller values of heating (Fig. 4).

The behavior of the chimney flow for various heating intensities of the airflow, in the limit case of equal far stagnation pressures (FSP) and for the three different models described is reproduced in Fig. 4, where the limiting, linear cases of the dynamic equilibrium are drawn through straight, tangent lines. These are in fact the derivatives of the mass flow rate in respect to r for the two limiting cases of heating.
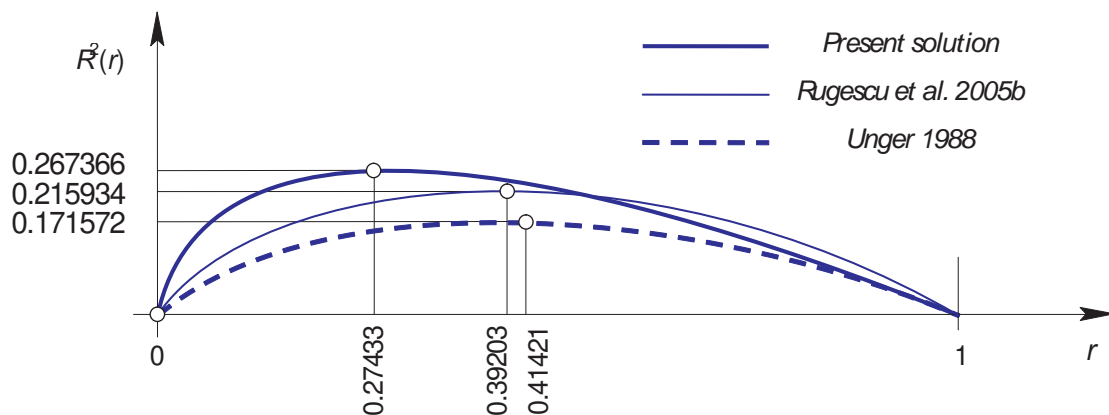

Figure 4. Stack discharge R^2 versus the air heating intensity r.

Differences between the present solution and the previous ones, as given in the above diagram, are non-negligible and show the sensible effect of the variation in modeling of the compressibility behavior at entrance and exit of the stack. This is explained by the tinny variations in pressure and density during the very small acceleration of the air at tower inlet that makes the flow highly sensible to pressure perturbations, either natural or numerical. The same applies for the tower exit. For this reason the previous solution was obtained by completely neglecting the air compressibility at tower upper exit, where the static pressure was taken into consideration instead of the dynamic one.

Numerical simulations of the ducted airflow and the experimental measurements on a scale model support of the present model. The conclusion of this very simplified but efficient modeling of the self-sustained gravity draught, with no energy extraction, is that the heating of the air must be limited to between 0.3÷0.5 in terms of the relative density reduction

through heating, or to between 90÷150ºC in terms of air temperature after heating, because under the accepted assumptions the product ϱT preserves almost constant. The optimal heating is thus surprisingly small. The maximum of function in Fig. 4 is flat and the minimal heating limit of 100ºC could be taken as sufficient for the best gravity draught acceleration. Recollection must be made that for the Manzanares green-house power station the air temperature increment was of 20ºC at maximal insolation only (Haaf 1984), fact that explains the failure of this project in demonstrating the ability of solar towers to produce electricity.

The accelerating potential and the expense of heat to perform this acceleration at optimal conditions result from equations (37)÷(39). In a practical manner, the velocity c_2 results in regard to the free-fall velocity (Torricelli) c_ℓ. Its upper margin is given by (40) through (37), while the lower margin by (41) through (38),

$$c_{2H} = \sqrt{\frac{r \cdot 2g\ell}{(1-r)[r(2-\Gamma)+\Gamma]}},$$ (40)

$$c_{2L} = \sqrt{\frac{r \cdot 2g\ell}{1-r^2}}$$ (41)

In fact these formulae render identical results for the optimal values for r (Table 1). For a contraction aria ratio of 10 the maximal airflow velocities in the test chamber c_e of the aeroacoustic tunnel versus the tower height are given in Table 1.

ℓ	c_ℓ	c_1	c_2	c_e
m	m/s	m/s	m/s	m/s
7	11.72	4.85	8.28	82.8
14	16.57	6.86	11.72	117.2
30	24.26	10.05	17.15	171.5
70	37.05	15.35	26.20	262.0
140	52.40	21.71	37.05	370.5

Table 1. Draught vs. tower height for a contraction ratio 10.

The value of c_e was computed according to the simple, incompressible assumption, which renders a minimal estimate for the air velocity in the contracted entrance area. Compressibility whatsoever will increase the actual velocity in the test area, while drag losses, especially those in the heat exchanger, will decrease that speed.

3. Experimental results

With the existing small-scale test rig built by the team of University "Politehnica" of Bucharest, the tests that have been conducted led to the values for air velocity in the tube as given in the diagram below. The average values, measured at a distance of 1.7 m from the entrance area of the tube, were registered as 2.115 m/s air speed with the contracted area effect (simulation of a turbine) and of 6.216 m/s without turbine simulation. Air temperature at the exit section was recorded to be of 195ºC and 123ºC, respectively (Tache et al. 2006).
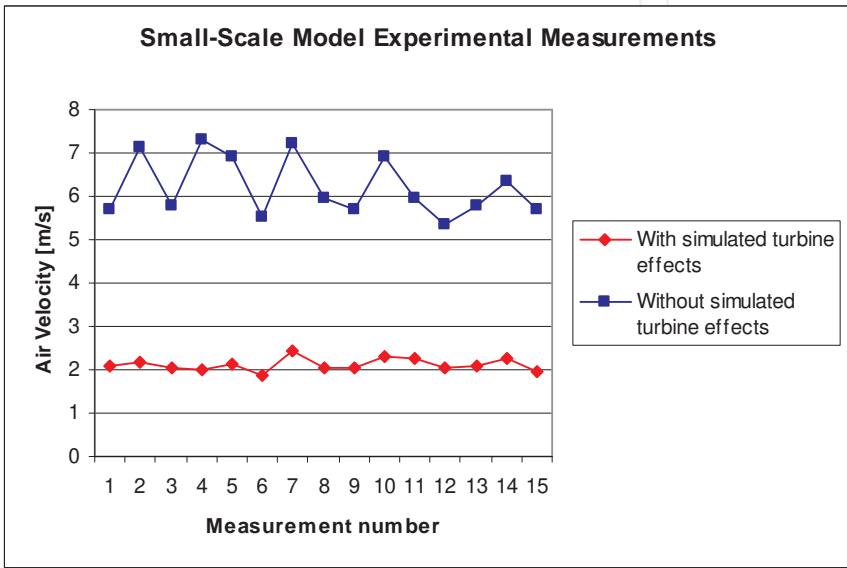

Figure 5. Experimental measurements on the small-scale model

The turbine simulation and the image of the inner electrical heater, simulating the solar receiver, are shown in figures below.
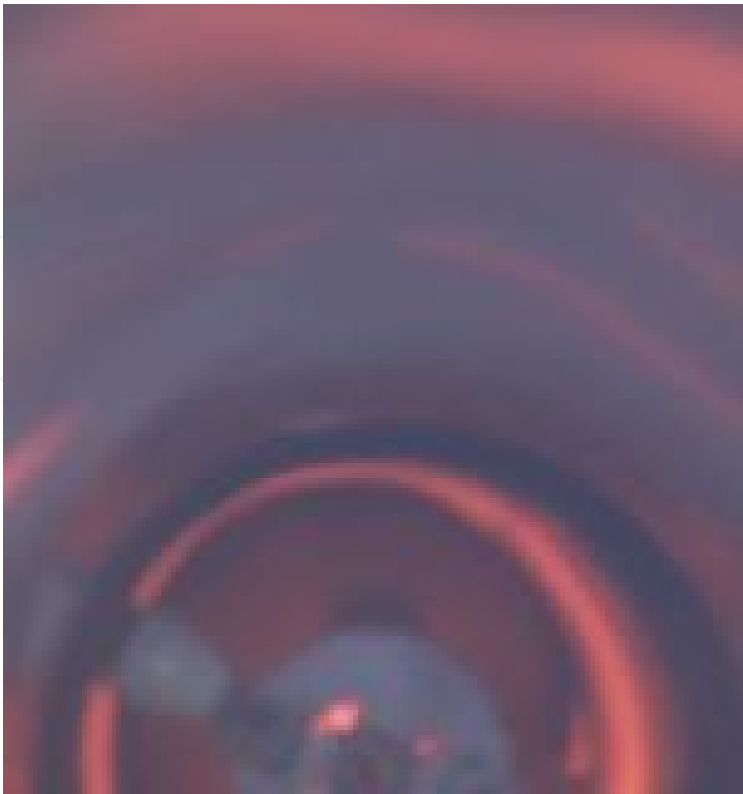

Figure 6. Turbine simulator

Figure 7. The air heater.

Figure 8. Small-scale model of the draught tower driver(overall view, ¼ contraction area, hot resistors, exit temperature)

The experimental values recorded during the measurement session and the ones obtained from numerical simulations are listed in Table 2.

No.	Measured Air Velocity [m/s]			Simulated Air Velocity [m/s]		
	With contraction	Without contraction	Speed Ratio	With contraction	Without contraction	Speed ratio
1	2.101	5.703	2.714			
2	2.190	7.110	3.247			
3	2.051	5.767	2.811	Vmin = 2.19	Vmin = 5.90	
4	1.996	7.310	3.662			
5	2.127	6.920	3.253			
6	1.867	5.521	2.957			
7	2.414	7.208	2.986			
8	2.027	5.966	2.943			
9	2.051	5.703	2.780			
10	2.307	6.920	3.000			
11	2.276	5.966	2.621	Vmax = 3.29	Vmax = 7.07	
12	2.027	5.351	2.639			
13	2.076	5.767	2.778			
14	2.276	6.329	2.780			
15	1.937	5.703	2.945			
Mean values	2.115	6.216	2.941	2.740	6.485	2.260

Table 2. Experimental and simulated air velocity values

The differences between these values are small, with greater values (~29.55%) when ac-counting for the turbine effects and much smaller values (~4.33%) in the other case.

4. Design example

As already stated, the optimal air heating for a good draught effect (Fig. 4) stays between $50 \div 100^{\circ}C$ and the computational problem is the following. Given the solar radiance flux, the reflectivity properties of the mirrors and the albedo of the tower walls, find the required area ratio of the solar reflector to the tower cross area that assures the imposed air heating. Considering the optional heating for a good mass flow-rate, formula (30) shows that, near the extreme pick, the discharge rate little depends on the heating intensity r. It was shown in (31) that the optimal rarefaction is placed around $r=0.4$, when the maximal discharge rate of $R^2=0.216$ manifests. Even at a moderate rarefaction of $r=0.14$ only, meaning a $50^{\circ}C$ tempera-ture rise above $27^{\circ}C$,

$$\frac{\rho}{\rho_0} \cong \frac{T_0}{T} = \frac{300}{350} \equiv 0.8571, \quad r \equiv 1 - \frac{\rho}{\rho_0} = 1 - 0.8571 \equiv 0.142857, \tag{42}$$

the discharge of the stack exhibits a good value of 2/3 of the maximal one,

$$R^2(r) \equiv \frac{r(1-r)}{1+r-\Gamma} = \frac{0.142857 \cdot 0.8571}{1+0.142857-0.288256} \equiv 0.1433 \tag{43}$$

At half of the optimal heating, that means at 100ºC, the discharge is comfortably up to 90% of the maximal one, or

$$R^2(r) \equiv \frac{r(1-r)}{1+r-\Gamma} = \frac{0.25 \cdot 0.75}{1.25-0.288256} \equiv 0.1950 \tag{44}$$

Under these circumstances it is fairly reasonable to accept for the further computation a moderate rarefaction of r=0.14 or 50ºC heating. With this value and the configuration in Fig. 2, meaning a 2-m internal diameter and again a tower height of 70 meters, the entrance velocity of the air becomes

$$w_1 \equiv \sqrt{2g\ell \cdot R^2} = \sqrt{1372.931 \cdot 0.1433} = 14.03 \ m/s, \tag{45}$$

where the density of the air is still the normal one ρ_0=1.225kg/m^3. Then the mass flow rate equals the value of

$$\dot{m} \equiv \rho_0 w_1 A = 1, 225 \cdot 14.03 \cdot 3.1415926 \equiv 54, 0 \ kg/s \tag{46}$$

Considering now a rough constant pressure specific heat of the air of

$$c_p = 1005 \ \frac{J}{kg \cdot K},$$

the power consumed with the heating of the air raises to

$$Q_1 \equiv \dot{m} \cdot c_p \cdot \Delta T = 54.0 \cdot 1005 \cdot 50 \equiv 2712498.3 \ W \tag{47}$$

Under a global heating efficiency of 80% the required total solar irradiation is

$$Q \equiv Q_1 / \eta = 2.7124983 / 0.8 \cong 3,39 \ MW \tag{48}$$

The lunar-averaged solar irradiation in Bucharest with the daily and annual values respectively are given below (University of Massachusetts 2004),

$$S = 3.87 \frac{kWh}{m^2 day} = 1414 \frac{kWh}{m^2 year},$$

for a local horizontal surface, under averaged turbidity conditions. From the ESRA database, the value of 3.7 results. In the same database, the optimal irradiation angle is given equal to 35º, although the local latitude is 45º. The difference is coming from the Earth inclination to the ecliptic. As far as the mirror system is optimally controlled, the radiation at the optimal angle must be accounted, as equal to:

$$S = 4.25 \frac{kWh}{m^2 day}, \tag{49}$$

and the mean diurnal insolation time at the same location in Bucharest equal to

$$t_S = 6.121 \quad \frac{h}{day} \tag{50}$$

The following solar irradiation intensity received during the daylight time results

$$Q_B \equiv \frac{S}{t_S} = \frac{4.25}{6.121} \equiv 0.6943 \quad \frac{kW}{m^2} \tag{51}$$

The reflector area, directly facing the Sun results, with the value of

$$A_S \equiv \frac{Q}{Q_B} = \frac{3390}{0.6943} \equiv 4882.4 \quad m^2 \tag{52}$$

Due to different angular positions of the mirrors versus the straight direction to the Sun, due to their individual location on the positioning circle, at least 50% extra reflector area is required to collect the desired radiating power from the Sun, or

$$A_R \equiv 1.5 \cdot A_S = 4882.4 \cdot 1.5 \equiv 7323.6 \, m^2 \tag{53}$$

When 3-m height mirrors are accommodated into circular rows of 200 meters diameter, that means a built surface of 1885 m^2 each, a number of 4 concentric rows must be provided to assure the required solar radiance on the draught tower, or 8 concentric semi-circle rows placed towards the north of the tower. The solution is materialized in Fig. 1. The provided power output must be considered when at least a 40% efficiency of the air turbine is involved, contouring a $2.71 \cdot 0.4 \cong 1 \, MW$ real output of the power-plant.

In contrast to the natural gravity air advent, when a turbine or other means of energy extraction are present, the characteristic of the tower suffers a major change however. The tower characteristic includes now the kinetic energy removal by the turbine under the form of externally delivered mechanical work.

5. Turbine effect over the gravity-draught acceleration

The turbine could be inserted after or before the air heater. For practical reasons, the turbine block is better imbedded right upwind the solar receiver (Fig. 9), forcing the raising of the position of the receiver and thus a better insolation of the heater along the whole daylight.

According to the design in Fig. 16, a turbine is introduced in the SEATTLER facility next to the solar receiver, with the role to extract at least a part of the energy recovered from the sun radiation and transmit it to the electric generator, where it is converted to electricity. The heat from the flowing air is thus transformed into mechanical energy with the payoff of a supplementary air rarefaction and cooling in the turbine. The best energy extraction will take place when the air recovers entirely the ambient temperature before the solar heating, although this desire remains for the moment rather hypothetical. To search for the possible amount of energy extraction, the quotient ω is introduced, as further defined. Some differences appear in the theoretical model of the turbine system as compared to the simple gravity draught wind tunnel previously described.
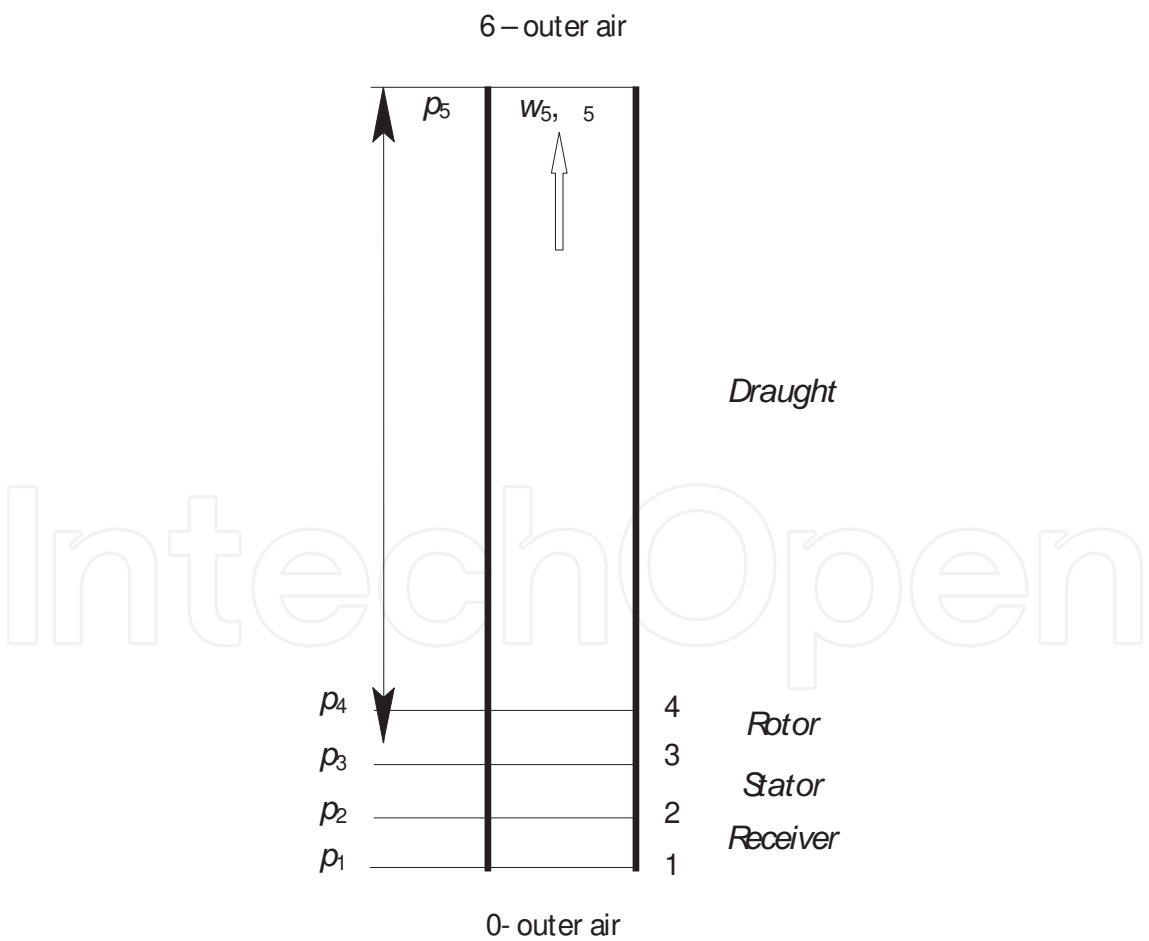

Figure 9. Main stations in the turbine cold-air draught tower.

To describe the model for the air draught with mechanical energy extraction we shall re-sume some of the formulas from above. First, the process of air acceleration at tower inlet is governed by the same incompressible energy (constant density ρ_0) equation,

$$p_1 = p_0 - \frac{\dot{m}^2}{2\rho_0 A^2} \tag{54}$$

The air is heated in the solar receiver with the amount of heat q, into a process with dilata-tion and acceleration of the airflow, accompanied by the usual pressure loss, called some-times as "*dilatation drag*" (Unger 1988). Considering a constant area cross-section in the heating solar receiver zone of the tube and adopting the variable r for the amount of heating rather than the heat quantity itself (19), with a given value for

$$\beta = \frac{T_1}{T_2} < 1, \tag{55}$$

the continuity condition shows that the variation of the speed is given by

$$c_2 = c_1 / \beta \tag{56}$$

No global impulse conservation appears in the tower in this case, as long as the turbine is a source of impulse extraction from the airflow. Consequently the impulse equation will be written for the heating zone only, where the loss of pressure due to the air dilatation occurs,

$$p_2 + \frac{\dot{m}^2}{\rho_2 A^2} = p_1 + \frac{\dot{m}^2}{\rho_0 A^2} - \Delta p_R \tag{57}$$

A possible pressure loss due to friction into the lamellar solar receiver is considered through Δp_R.

The dilatation drag is thus perfectly identified and the total pressure loss Δp_Σ from outside up to the exit from the solar heater is present in the expression

$$p_2 = p_0 - \frac{\dot{m}^2}{2\rho_0 A^2} - \frac{\dot{m}^2}{\rho_2 A^2} + \frac{\dot{m}^2}{\rho_0 A^2} - \Delta p_R \equiv p_0 - \Delta p_\Sigma \tag{58}$$

Observing the definition of the rarefaction factor in (54) and using some arrangements the equation (58) gets the simpler form

$$p_2 = p_0 - \frac{\dot{m}^2}{\rho_0 A^2} \cdot \frac{r+1}{2(1-r)} - \Delta p_R \tag{59}$$

The thermal transform further into the turbine stator grid is considered as isentropic, where the amount of enthalpy of the warm air is given by

$$q = \frac{p_1}{\rho_1} \cdot \frac{1-\beta}{\beta} + \frac{\dot{m}^2}{\rho_1^2 A^2} \cdot \left[\frac{1-\dfrac{\Gamma}{2}\beta}{\beta} + \frac{\dfrac{\Gamma}{2}-1}{\beta^2} \right] - \frac{\Delta p_R}{\rho_1} \cdot \frac{1}{\beta}$$

If the simplifying assumption is accepted that, under this aspect only, the heating progresses at constant pressure, then a far much simpler expression for the enthalpy fall in the stator appears,

$$\Delta h_{23} = \omega q = \omega c_p T_2 r \tag{60}$$

To better describe this process a choice between a new rarefaction ratio of densities ρ_3/ρ_2 or the energy quota ω must be engaged and the choice is here made for the later. Into the isentropic stator the known variation of thermal parameters occurs,

$$\frac{T_3}{T_2} = 1 - \omega r, \tag{61}$$

$$\frac{p_3}{p_2} = (1 - \omega r)^{\frac{\kappa}{\kappa - 1}}, \tag{62}$$

$$\frac{\rho_3}{\rho_2} = (1 - \omega r)^{\frac{1}{\kappa - 1}} \tag{63}$$

The air pressure at stator exit follows from combining (62) and (59) to render

$$p_3 = \left[p_0 - \frac{\dot{m}^2}{\rho_0 A^2} \cdot \frac{r+1}{2(1-r)} - \Delta p_R \right] (1 - \omega r)^{\frac{\kappa}{\kappa - 1}} \tag{64}$$

Considering the utilization of a Zölly-type turbine, its rotor wheel keeps thermally neutral by definition and thus no variation in pressure, temperature and density appears in the rotor channel. The only variation is in the direction of the air motion, preserving its kinetic energy as constant.

Thus the absolute velocity of the airflow decreases from the value c_3 to the value $c_3 \sin \alpha_1$ and this kinetic energy variation is converted to mechanical work delivered outside. Consequently $\rho_4 = \rho_3$, $p_4 = p_3$, $T_4 = T_3$ and thus the local velocity at turbine rotor exit is given by

$$c_4 = \frac{c_1}{(1-r)(1-\omega r)^{\frac{1}{\kappa - 1}}} \tag{65}$$

The air ascent in the tube is only accompanied by the gravity up-draught effect due to its reduced density, although the temperature could drop to the ambient value. We call this quite strange phenomenon the *cold-air draught*. It is governed by the simple gravity form of Bernoulli's equation of energy,

$$p_5 = p_3 - g\rho_3\ell \qquad (66)$$

The simplification was assumed again that the air density varies insignificantly during the tower ascent. The value for p_3 is here the one in (65). At air exit above the tower a sensible braking of the air occurs in compressible conditions, although the air density suffers insignificant variations during this process.

The energy equation in the form of Bernoulli is used to retrieve the stagnation pressure of the moving air above the upper exit from the tower, under incompressible condition when the density remains constant,

$$p_6{}^* = p_5 - \frac{\Gamma}{2}\rho_5 c_5{}^2 = p_5 + \frac{\Gamma}{2} \cdot \frac{\dot{m}^2}{\rho_3 A^2} = p_5 + \frac{\Gamma}{2} \cdot \frac{\dot{m}^2}{\rho_0 A^2} \cdot \frac{\rho_0}{\rho_3} \qquad (67)$$

Value for p_5 from (66) and for the density ratio from (54) and (63) are now used to write the full expression of the stagnation pressure in station "6" as

$$p_6{}^* = (p_0 - \Delta p_R)(1-\omega r)^{\frac{\kappa}{\kappa-1}} - \frac{\dot{m}^2}{\rho_0 A^2} \cdot \frac{r+1}{2(1-r)} \cdot (1-\omega r)^{\frac{\kappa}{\kappa-1}} + \frac{\dot{m}^2}{\rho_0 A^2} \cdot \frac{\Gamma}{2} \cdot \frac{1}{(1-r)\cdot(1-\omega r)^{\frac{1}{\kappa-1}}} - g\rho_4\ell \qquad (68)$$

It is observed again that up to this point the entire motion into the tower hangs on the value of the mass flow-rate, yet unknown. The mass flow-rate itself will manifest the value that fulfils now the condition of outside pressure equilibrium, or

$$p_6{}^* = p_0 - g\rho_0\ell \qquad (69)$$

This way the air pressure at the local altitude of the outside atmosphere equals the stagnation pressure of the escaping airflow from the inner tower. Introducing the equation (68) in equation (69), after some re-arrangements of the terms, the dependence of the global mass flow-rate along the tower, when a turbine is inserted after the heater, is given by the developed formula:

$$R^2(\gamma) \equiv \frac{\dot{m}^2}{2g\ell\rho_0^2 A^2} = \frac{1-r}{(r+1)(1-\omega r)^{\frac{\kappa+1}{\kappa-1}} - \Gamma}\left\{(1-\omega r)^{\frac{1}{\kappa-1}} + \frac{p_0}{g\rho_0\ell}\left[(1-\omega r)^{\frac{\kappa}{\kappa-1}}-1\right] - \frac{\Delta p_R}{g\rho_0\ell}(1-\omega r)^{\frac{\kappa}{\kappa-1}}\right\} \qquad (70)$$

where the notations are again recollected

$r = \dfrac{\rho_0 - \rho_2}{\rho_0}$, the dilatation by heating in the heat exchanger, previously denoted by r;

ω = the part of the received solar energy which could be extracted in the turbine;
Δp_R = pressure loss into the heater and along the entire tube either.

All other variables are already specified in the previous chapters. It is clearly noticed that by zeroing the turbine effect ($\omega = 0$) the formula (70) reduces to the previous form in (37), or by neglecting the friction to (38), which stays as a validity check for the above computations.

For different and given values of the efficiency ω the variation of the mass flow-rate through the tube depends of the rarefaction factor r in a parabolic manner.

6. Discussion on the equations

Notice must be made that the result in (70) is based on the convention (60). The exact expression of the energy q introduced by solar heating yet does not change this result significantly. Regarding the squared mass flow-rate itself in (70), it is obvious that the right hand term of its expression must be positive to allow for real values of R^2. This only happens when the governing terms present the same sign, namely

$$\left\{(r+1)(1-\omega r)^{\frac{\kappa+1}{\kappa-1}} - \Gamma\right\} \cdot \left\{1-(1-r)(1-\omega r)^{\frac{1}{\kappa-1}} + \frac{p_0}{g\rho_0\ell}\left[(1-\omega r)^{\frac{\kappa}{\kappa-1}}-1\right] - \frac{\Delta p_R}{g\rho_0\ell}(1-\omega r)^{\frac{\kappa}{\kappa-1}}\right\} : 0 \qquad (71)$$

The larger term here is the ratio $p_0/(g\rho_0\ell)$, which always assumes a negative sign, while not vanishing. The conclusion results that the tower should surpass a minimal height for a real R^2 and this minimal height were quite huge. Very reduced values of the efficiency ω should be permitted for acceptably tall solar towers. This behavior is nevertheless altered by the first factor in (71) which is the denominator of (60) and which may vanish in the usual range of rarefaction values r. A sort of thermal resonance appears at those points and the turbine tower works properly well.

7. Discussion on denominator

The expression from the denominator of the formulae (70), which gave the flow reportedly, it can be canceled (becomes 0) for the usual values of the dilatation rapport (ratio) gamma and respectively quota part from energy extracted omega. This strange behavior must be explained. The separate denominator in (72) is,

$$A \equiv \left\{(r+1)(1-\omega r)^{\frac{\kappa+1}{\kappa-1}} - \Gamma\right\} = 0 \qquad (72)$$

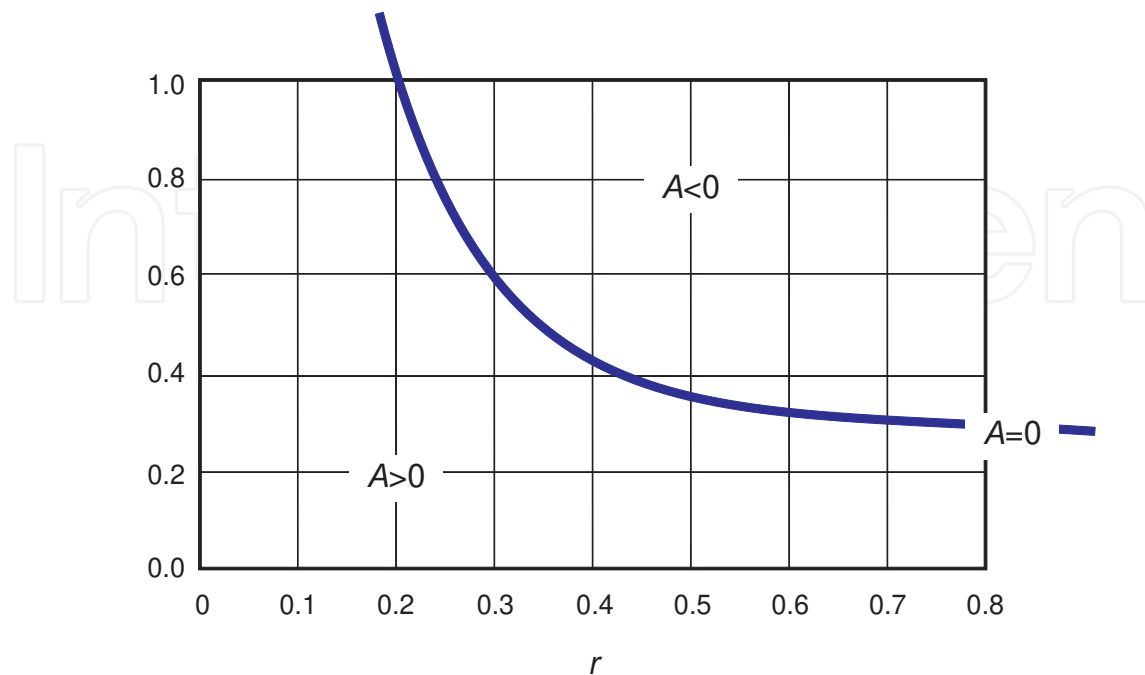The curve of zeros and the zones with opposite signs are:

Figure 10. The denominator zeros from (71)

It is yet hard to accept that such a self-amplification or pure resonance of the flow can be real and in fact the formulae (71) does not allow, in its actual form, the geometrical scaling of the tunnel and of the turbine. The rigor of computational formulae is out of any discussion, this showing that the previous result outcomes from the hypotheses adopted. Among those, the hypothesis of isobaric heating before the turbine is obviously the most doubtful.

8. Improved model

Analyzing the simple draught only, observe how easily the hypothesis of isobaric heating leads to an incomplete result, by eliminating the drag produced by the thermal dilatation and the acceleration throw heating, thus reducing the problem to a linear one, without physical anchorage. It could be presumed that the acceptance of relation (57) for the cooling in the stator, relation where it was presumed that the anterior heating performed isobaric, induces an excessive rigidity in the computational model. Replacing this very simple relation between the temperatures and the heat added to the fluid through a non-isobaric relation complicates drastically the model, which becomes completely nonlinear.

It remains to be analyzed whether such an inconvenient model leads to physically acceptable results for the values of mass flow-rate in the turbine tower.

The isobaric relation (60) will be replaced by the exact equation,

$$\Delta h_{23} \equiv c_p T_2 \left(1 - \frac{T_3}{T_2}\right) = \omega q(r), \tag{73}$$

where the heat received in non isobaric heat exchanger is expressed, through the equation of energy, in the complete form:

$$q(r) = c_p T_0 \frac{r}{1-r} - \left(1 - \frac{\Gamma}{2}\right) \cdot \frac{\gamma}{\Gamma(1-r)^2} \cdot \frac{\dot{m}^2}{\rho_0^2 A^2} - \frac{\Delta p_R}{\Gamma(1-r)\rho_0}, \tag{74}$$

to take also into account the possible pressure losses due to friction in the solar receiver Δp_R.

The absorbed heat (74) will also be used in its complete form in the relation that supplies the pressure at stator exit:

$$\frac{p_3}{p_2} = \left(1 - \omega \frac{q}{c_p T_2}\right)^{\frac{\kappa}{\kappa-1}}, \tag{75}$$

fact that obviously induces another level of non-linearity. Using also the equation of state, the pressure from the stator exits writes from (71),

$$p_3 = p_2^{-\frac{1}{\kappa-1}} \left[p_2 - \omega \left(r\, p_0 - \frac{2-\Gamma}{2} \cdot \frac{r}{1-r} \cdot \frac{\dot{m}^2}{\rho_0 A^2} - \Delta p_R\right) \right]^{\frac{\kappa}{\kappa-1}}, \tag{76}$$

and for the value p_2 the pressure losses from the entrance through Bernoulli acceleration and in the heater will be now respectively inferred,

$$p_2 = p_0 - \frac{\dot{m}^2}{\rho_0 A^2} \left(\frac{\Gamma}{2} + \frac{r}{1-r}\right) - \Delta p_R \tag{77}$$

Taking into account the draught from the tower (66) and the fluid brake at exit (67), the equilibrium of static pressure reads

$$(p_2 - \omega \beta \chi\, p_0)^{\frac{2}{\kappa-1}} \left[\frac{(p_2 - \omega \beta \chi\, p_0)^\kappa}{g \rho_0 \ell} - \beta\right] + \frac{\Gamma}{2} \frac{\dot{m}^2}{\rho_0^2 A^2 g \ell \beta} p_2^{\frac{2}{\kappa-1}} + (1-\pi)[p_2(p_2 - \omega \beta \chi\, p_0)]^{\frac{1}{\kappa-1}} = 0 \tag{78}$$

Here the notation was used:

$$\pi = \frac{p_0}{g\, \rho_0 \ell} >> 1 \tag{79}$$

In the followings the undimensionalised flow-rate D^2 will be considered as the solving variable of the problem, a variable that naturally appears from the previous equation (78), under the form of the ratio

$$D^2 \equiv \frac{R^2}{\pi} = \frac{\dot{m}^2}{2\rho_0^2 A^2 g\ell} \cdot \frac{g\rho_0\ell}{p_0} = \frac{c_1^2}{2RT_0} \equiv \left(\frac{c_1}{c_0}\right)^2, \tag{80}$$

where also naturally appears the characteristic velocity c_0 of the air c_0, namely

$$c_0 \equiv \sqrt{2RT_0} \approx 415,5 \; m/s \tag{81}$$

The characteristic velocity c_0 is actually related to the local sound velocity in the air a_0, manifesting proportional to it, so that the relative mass flow-rate can be written in the absolutely equivalent form,

$$a_0 \equiv \sqrt{\kappa R T_0} \approx 348,2 \; m/s \tag{82}$$

in connection with which the relative flow-rate couls also be expressed, in the form

$$D^2 \equiv \frac{R^2}{\pi} = \frac{\kappa}{2} \frac{c_1^2}{a_0^2} \equiv \frac{\kappa}{2} M_1^2, \tag{83}$$

in other words this flow-rate is proportional to the squared local Mach number of the flow.

From (78) the equation of the flow-rate D^2 is obtained as a function of the working conditions, expressed through the parameters ω and r,

$$(a \cdot c - b D^2)^5 [(c - b D^2)^{1,4} - c^{2,4}] + d \cdot c^{0,4} D^2 (c - e D^2)^5 + f \cdot c^{1,4} (c - e D^2)^{2,5} (a \cdot c - b D^2)^{2,5} = 0 \tag{84}$$

where the constant coefficients are again reproducing those working conditions,

$$\begin{aligned} a &\equiv 1 - \omega r, & e &\equiv 2r + \Gamma(1-r), \\ c &\equiv 1 - r, & d &\equiv \Gamma\pi, \\ f &\equiv 1 - \pi, & b &\equiv e - \omega r(2 - \Gamma). \end{aligned} \tag{85}$$

The algebraic, non linear equation (80) is now solved using a standard numerical method to obtain solutions for the mass flow-rate, as depending on the different working conditions concerning the heating level applied in the solar receiver r and respectively the degree of recovery of the heat introduced through the receiver ω. For a complete recovery of energy ($\omega=1$), the numerical solutions are given in the following table (Table 3):

It proves however that the above given model is not properly reproducing the Stack-Turbine (S-T) characteristic at low heating rates ($r \to 0$), while at the upper end ($r \to 1$) it acceptably does this. The same improper behavior is observed when for example a compressible, variable density acceleration at the stack entrance is considered in the simple draught. In that case the "false" equation appears,

$$\frac{\dot{m}^2}{2g\ell\,\rho_0{}^2A^2} = 1 - r,$$ (86)

or

$$D^2 - (1-r)/\pi = 0$$ (87)

A very slight change in the assumptions could therefore deeply affect the result of the simulation modeling, due to the small overall magnitudes of pressure and density gradients along the S-T channel.

r	D²
0	3,50
0,1	-
0,2	(1,280)
0,3	(0,875)
0,4	0,611331000
0,5	0,428261326
0.6	0,298397500
0,7	0,199248700
0,8	0,1098315 şi 0,012898027
0,9	0,0634500 şi 0,055130000
1,0	0,00

Table 3. The equilibrium flow-rate as a function of the rarefaction γ for ω=1

The results are plotted in the diagram from Fig. 11. The discharge characteristic of the tunnel resulting from the given assumptions is drawn in dark red.
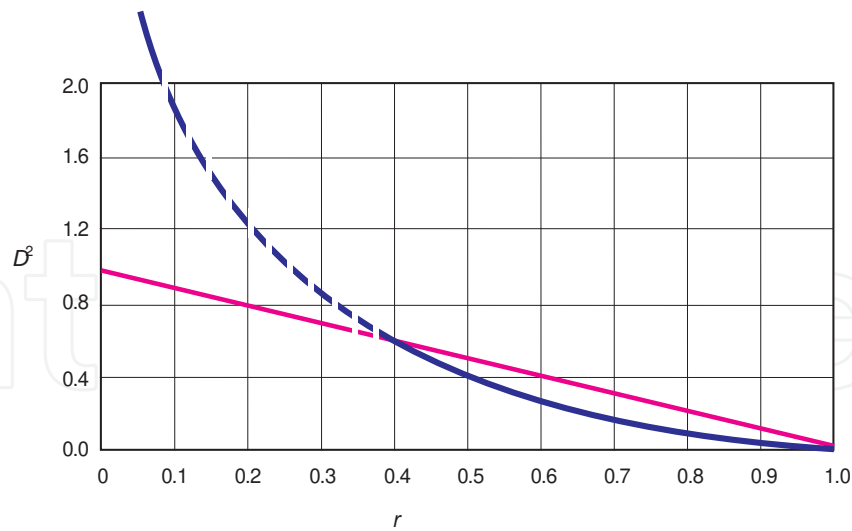
Figure 11. Discharge characteristic of SEATTLER tower.

9. Energy output of the gravity-draught accelerator

The main concern and reluctance for the classical solar towers comes from the regular per-ception that the energetic efficiency of those systems is unsatisfactory. Largely correct, this perception does not further stand valid for gravity draught towers and to prove this a piece of attention must be allocated to the energy balance.

The equation of energy in its rough form (3) needs thus further attention. Pointing the val-ues to the exit station "2" of the receiver (Fig. 2) we first observe that the gain in kinetic ener-gy e_g given by the tower directly, per kilogram of air, defined by

$$e_g \equiv \frac{w_2^2}{2}$$

is equal to

$$e_g = q - g(z_2 - z_1) - c_p(T_2 - T_0) \tag{88}$$

where the first right-hand term is the total heat introduced into the stack per one kg of air, and the last term represents the heat consumed for directly heating the air to the final tem-perature T_2. The second term, which acts as a reducer of the efficiency, is relatively small in comparison to the others.

The quantity of kinetic energy transferred to the air is the difference that remains available. This entire amount could be used to produce energy, without any thermal or mechanical loss. Physically, the heat introduced in the air to create the up-draught along the tower could entirely be extracted into useful mechanical work through a low temperature wind

turbine, and the draught is maintained due to the low air density despite the energy extraction in the tower.

The process remains however greatly dependent to the optimal selection of the heating level and of the utilization of the solar radiation in an efficient manner. The problem with the cloudy weather and the energy stocking during the night are solved through heat accumulators of specific construction.

10. Conclusion

The principle of a solar energy power plant, based on a mirror-type collector, is depicted in the nearby drawing. It represents the application of the WINNDER thermal accelerator principle into the ecological and sustainable means of accelerating the air without any moving device and, consequently, with a very low noise and turbulence level, ideal for aeroacoustic applications. A multiple-rows array of controllable ground mirrors are installed around. In this manner a highly efficient utilization of the solar energy is available, due to the known high release coefficient of the mirror surfaces. Means to follow the Sun along its apparent trajectory are common and available at low cost today. Problems regarding the maintenance of the system can be solved through a proper technological and economic management of the facility.

It does not seem however equally attractive for energy production, despite the clean method involved, but this represents a first sight impression, easily dismounted through an in-depth analysis. The computational model depicted above shows that the resources for producing energy trough the solar gravity draught are high enough and represent an interesting resource of green energy of a new and yet unexplored type.
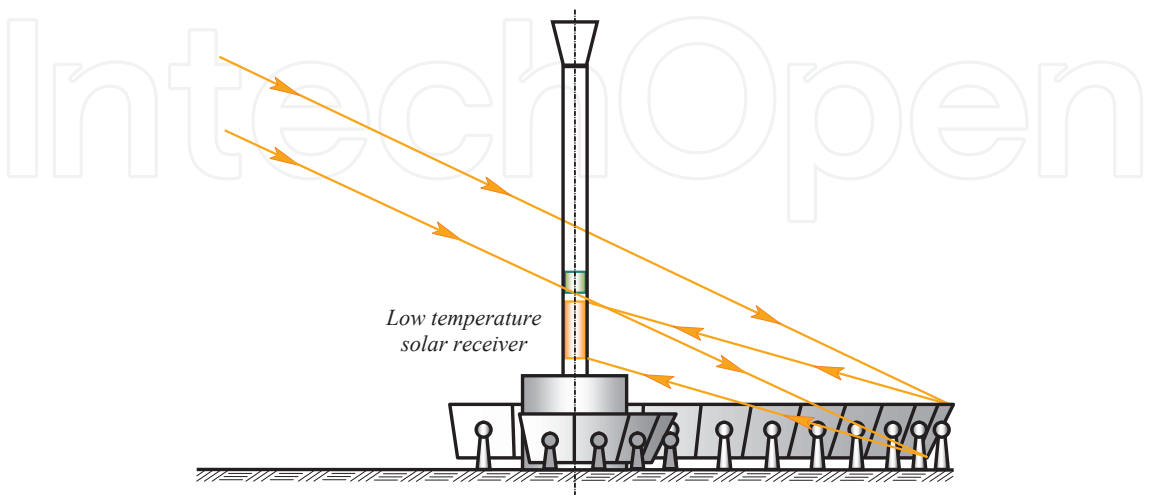

Low temperature solar receiver

Figure 12. Principle of WINNDER concentrator for aeroacoustic applications.

Although the equipment costs of the present project are much higher than the Greenhouse power plant ones, it is believed that the overall costs are still competitive and the proposed solution of reflector tower is useful. One of the explanations resides in the fact that the reflexivity of the mirrors is very high. The design example given above highlights the main factors.
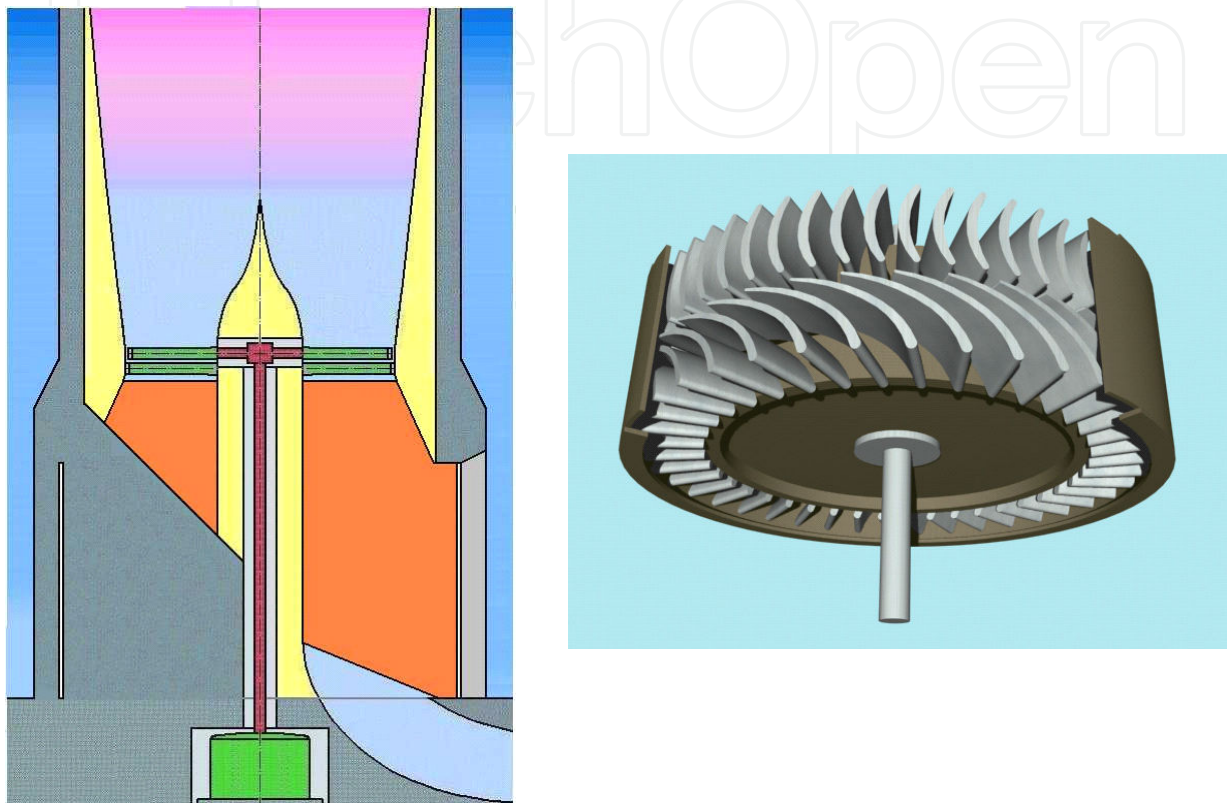

Figure 13. STRAND air turbine.

This example shows that a circular ground surface of roughly 0.8 *ha* at maximum must be used to produce a 1 *MW* power output, or 0.8 *ha*/*MW*. The figure is to be compared to the one of Manzanares power-plant in Spain, built under the solar green-house collector program, where the amount of occupied soil equals 90 *ha*/*MW* or 100 times more (peak output of 50 *kW* for a collector diameter of 240 meters). This capacity is also higher than the surface-to-power production intensity of photoelectric cells of 1.0 *ha*/*MW* (Energy Form EIA-63B). The costs of Solar cells of 4.56 *$*/*PeakW* (1995) are still high.

After the data in (Schleich et al. 2005) this value equals 0,94 and this adds to the very high absorbing properties of the tower walls. It serves here as a nice illustration of possible extra applications of the chimney draught effects in directly producing electrical power.

As another comparison item, the newly renovated Solar Two solar thermal electric generating station, located in California's Mojave Desert, consists of 1,900 motorized mirrors surrounding a generating station with 10 megawatts of capacity, which began operation in early 1996. It is part of an effort to build a commercially viable 100-*MW* solar thermal system

by 2000 (Energy 1997). The 10-MW Solar Two solar thermal electric plant near Barstow, CA, began operation in early 1996 on the site of the Solar One plant. Solar Two differs from Solar One primarily in that it includes a molten-salt storage system, which allows for several hours of base-load power generation when the sun is not shining.

The molten salt (an environmentally benign combination of sodium nitrate and potassium nitrate) allows a summer capacity factor as high as 60%, compared with 25% without storage. The plant consists of 1,926 motorized mirrors focused on a 300-*ft*-high central receiver generating station rated at 10 *MW*. Molten salt from the "cold" salt tank (at 550ºF) is heated to 1,050ºF and stored in the "hot" salt tank. Later the hot salt is passed through a steam generator to produce steam for a conventional steam turbine.

Equipment costs of WINNDER are higher than for the Greenhouse power plants, still the overall costs of exploitation and maintenance are competitive and the proposed combination of mirror array and draught tower is literally efficient. It remains to convince the investors of the efficiency of this exotic energy producer.

The gravitational up-draught due to Archimedes's effect does not contribute, in any way, to the balance of energy. It simply remains the driver of the air into the stack and the solar energy introduced in the system is the only source of air acceleration and further production of electric energy within a turbo-generator. Consequently it does not seem specifically attractive for energy production, although it provides the cleanest energy ever and involves the lowest levels of losses.

Author details

Radu D. Rugescu[*]

Address all correspondence to: rugescu@yahoo.com

University "Politehnica" of Bucharest, Romania

References

[1] Bejan, A., Convection Heat Transfer, New York, Wiley and Sons, 1984.

[2] Cirligeanu, R., Rugescu, R. D., and AlinaBogoi (2010), TRANSIT code for turbine flows in solar-gravity draught power plants, Paper GT2010-22518, Proceedings of the ASME International Conference on Gas Turbines, June 14-18, 2010, Glasgow, Skotland, UK.

[3] Gannon, A. J., T. W. Von Backström, Solar Chimney Turbine Performance, ASME Journal of Solar Energy Engineering, 125, 2003, p101-106.

[4] Haaf, W., Solar Chimneys, Part II: Preliminary Test Results from the Manzanares Pilot Plant, Int. J. Sol. Energy, 2 (1984), pp. 141–161.

[5] Jaluria, Y., Natural Convection, Heat and Mass Transfer, Oxford, New York, Pergamon Press, 1980.

[6] Mancini, Th. R., Solar-Electric Dish Stirling System Development, SAND-97-2924C, 1998.

[7] Mueller R.W., Dagestad K.F., Ineichen P., Schroedter M., Cros S., Dumortier D., Kuhlemann R., Olseth J.A., Piernavieja G., Reise C., Wald L., Heinnemann D. (2004), Rethinking satellite based solar irradiance modelling - The SOLIS clear sky module. Remote Sensing of Environment, 91, 160-174.

[8] Raiss, W., Heiz- und Klimatechnik, Springer, Berlin, vol. 1, pp. 180-188, 1970.

[9] Rugescu, R. D., ThermischeTurbomaschinen, ISBN 973-30-1846-5, E. D-P. Bucharest 2005.

[10] Rugescu, R. D., T. G. Chiciudean, A. C. Toma, F. Tache, Thermal Draught Driver Concept and Theory as a Tool for Advanced Infra-Turbulence Aerodynamics, in DAAAM Scientific Book 2005, ISBN 3-901509-43-7 (Ed. B. Katalinic), DAAAM International Viena, 2005.

[11] Rugescu, R. D., D. A. Tsahalis, and V. Silivestru (2006), Solar-Gravity Power Plant Modeling Uncertainties, WSEAS Transactions on Power Systems, ISSN 1790-5060, 10(2006), pp.1713-1720.

[12] Rugescu, R. D. (2008), "Technology of CFD in space engines and solar-gravitational power plants", International Journal on Energy Technology and Policies, ISSN 1472-8923, On-line ISSN 1741-508X, 6, 1-2(2008), p.124-142.

[13] Rugescu, R. D., Silivestru V., and Ionescu M. D. (2008),Technology of Thermal Receivers and Heat Transfer for SEATTLER towers, Chapter 59 in the DAAAM International Scientific Book 2008, pp. 697-742, B. Katalinic (Ed.), published by DAAAM International Vienna, ISBN 3-901509-69-0, ISSN 1726-9687, Vienna, Austria.

[14] Rugescu, D. R. and R. D. Rugescu (2009), Chapter 1 "Potential of the solar energy on Mars", pp. 01-24, in Rugescu, D. R. (editor), "Solar Energy", ISBN 978-953-307-052-0, Ed. INTECH, Rjeka, Croatia, 2010, 462 p.

[15] Rugescu, R. D., R. B. Cathcart, Dragos R. Rugescu, and S. P. Vataman (2010), Electricity and Freshwater Macro-project in the Arid African Landscape of Djibouti, ARGEO-C3 Conference, Exploring and harnessing the renewable and promising geothermal energy, 22-25 November, Djibouti.

[16] Rugescu, R. D., R. B. Cathcart, and Dragos R. Rugescu, Electricity and Freshwater Macro-project in an Arid, Ochre African Landscape: Lac Assal (Djibouti), Eighth International Conference on Structural Dynamics, Proceedings EURODYN-2011, Leuven, Belgium, 4-6 July 2011 (pp NA).

[17] Rugescu, R. D., A. Bogoi, and R. Cirligeanu (2011), Intricacy of the TRANSIT manifold concept paid-off by computational accuracy, Proceedings of ICMERA-2011 Conference, ISBN 978-981-07-0420-9, ISSN 2010-460X, Bucharest 20-22 October, Romania, pp. 61-65.

[18] Rugescu, R. D. (Ed.), Solar Power, ISBN 978-953-51-0014-0, INTECH Press, Rjeka, Croatia, Hard cover, 378 pages, Feb. 2012.

[19] Rugescu, R. D., and C. Dumitrache (2012), Solar Draught Tower Simulation and Proof by Numerical-Analytical Methods, Paper V&V2012-6191, ASME 2012 Verification and Validation Symposium, Las Vegas, May 2-4, 2012, p. 73.

[20] Rugescu, R. D., Demos T. Tsahalis, CiprianDumitrache (2012), Extremely High Draught Tower Efficiency Proof by Conservation of Energy, Invited plenary lecture, Proceedings of the 5th IC-SCCE 2012 From Scientific Computing to Computational Engineering, 4-7th July 2012, Athens, Greece, pp. 243-248.

[21] Scharmer, K., Greif, J. (2000), The European Solar Radiation Atlas, Presses de l'Ecole des Mines, Paris, France.

[22] Schiel, W., T. Keck, J. Kern, and A. Schweitzer, Long Term Testing of Three 9 kW Dish-Stirling Systems, ASME International Solar Energy Conference, San Francisco, CA, USA, March 1994.

[23] SchleichBergermann und Partners (2005), EuroDish System Description.

[24] Tache, F., Rugescu, R. D., Slavu, B., Chiciudean, T. G., Toma, A. C., and Galan, V. (2006), Experimental demonstrator of the draught driver for infra-turbulence aerodynamics, Proceedings of the 17th International DAAAM Symposium, "Intelligent Manufacturing & Automation: Focus on Mechatronics & Robotics", Vienna, 8-11th November 2006.

[25] Unger, J., Konvektionsströmungen, B. G. Teubner, ISBN 3-519-03033-0, Stuttgart, 1988.

[26] Energy Information Administration, Form EIA-63B, "Annual Photovoltaic Module/ Cell Manufacturers Survey."

[27] Energy Information Administration, Office of Coal, Nuclear, Electric and Alternate Fuels, Renewable Energy Annual 1996, U.S. Department of Energy, Washington, DC 20585, April 1997.

[28] University of Massachusetts (2004), Lowell Photovoltaic Program, International Solar Irradiation Database, Version 1.0, Monthly solar irradiation.